Ball Grid Array Reliability Assessment for Aerospace Applications

Reza Ghaffarian, Ph.D.
Jet Propulsion Laboratory
California Institute of Technology
(626) 354-2059

Narnsoo P. Kim, Ph.D.
Boeing Defense & Space Group
(253) 657-5970

Abstract

Reliability of Ball Grid Arrays (BGAs) was evaluated with special emphasis on space applications. This work was performed as part of a consortium led by the Jet Propulsion Laboratory (JPL) to help build the infrastructure necessary for implementation of this technology. Nearly 200 test vehicles, each with four packages, were assembled and tested using an experimental design. The most critical variables incorporated in this experiment were package type, board material, surface finish, solder volume, and environmental condition, The packages used for this experiment were commercially available packages with over 250 I/Os including both plastic and ceramic BGA packages.

The test vehicles were subjected to thermal and dynamic environments representative of aerospace applications. Two different thermal cycling conditions were used, the JPI. cycle ranged from -30 "C to 100 "C and the Boeing ranged from -55 "C to 125 "C. The test vehicles were monitored continuously to detect electrical failure and their failure mechanisms were also characterized. They were removed periodically for optical inspection, Scanning Electron Microscopy (SEM) evaluation, and cross-sectioning for crack propagation mapping. Data collected from both facilities were analyzed and fitted to distributions using the Weibull distribution and Coffin-Manson relationships for failure projection. This paper will describe experimental results as well as those analyses.

Introduction

BGA is an important technology for utilizing higher pin counts, without the attendant handling and processing problems of the peripheral array packages. They are atso robust in processing because of their higher pitch (0.050 inch typical), better lead rigidity, and self-alignment characteristics during reflow processing.

BGAs' solder joints cannot be inspected and reworked using conventional methods and are characterized well for multiple double sided assembly processing methods. In ultra low and low volume SMT assembly applications, e.g. space and defense, the ability to inspect the solder joints visually has been standard and has been a key factor for providing confidence in solder joint reliability.

To address many common quality and reliability issues of BGAs, JPL organized a consortium with sixteen members in early 1995[1]. Diverse membership from military, commercial, academia, and infrastructure sectors allowed in a concurrent engineering approach to resolve many challenging technical issues. This paper will present the most current experimental results for the test vehicles assembled under this consortium. The board level thermal cycling data for ceramic packages with 625 1/0, plastic packages with 313 1/0 and 352 1/0s will be presented. Analysis and testing of other assemblies are being carried out and will be presented in a future paper.

Test Vehicle Configuration

Two test vehicle assemblies included plastic and ceramic packages. Both FR-4 and polyimide

Printed Wiring Boards with 6 layers, .062 inch thick, were used.

Plastic packages cover the range from OMPAC to SuperBGAs (SBGAs). These were:

. Two Peripheral SBGA, 352 and 560 1/0
- Peripheral OMPAC 3521/0, PBGA 352 and 256
- DepopulatedPBGA313 I/Os

. 256 QFP, 0.4 mm Pitch

In SBGA, the IC die is directly attached to an oversize copper plate providing a better heat dissipation efficiency. The solder bails for plastic packages are eutectic (63 Sn/37Pb).

Ceramic packages with 625 1/0s and 361 1/0s were also include in our evaluation. Ceramic solder bails have 0.035 inch diameters and have a high melting temperature (90Pb/10Sn). These balls are attached to the ceramic substrate with eutectic solder (63 Sn/37Pb) material. At reflow, package eutectic solder and the PWB eutectic paste reflow to provide the electro-mechanical interconnects.

Plastic packages had dummy dies within their range of cavities. All packages had daisy chains and the daisy chain on PWB designed such to be able to monitor critical regions. Most packages had four daisy chain patterns, 5601/0 had five, and QFP had one.

Package Dimensional Characteristics

Package dimensional characteristics are among the key variables that affect solder joint reliability. Dimensional characteristics of all packages were measured using a 3D laser scanning system. Output metrics included solder bail diameter, package warpage, and coplanarity[2].

Test Vehicle Assembling

Full assembling was implemented after process optimization from the trial test. The following procedures were followed:

- PWBS were baked at 125°C for 4 hours prior to screen printing.
- Two types of solder pastes were used, an RMA and a water soluble one.
- Pastes were screen printed and the heights were measured by laser profilometer. Three levels of paste were included in evacuation: Standard, high, and iow. Stencils were stepped to 50% to accommodate assembling of ceramic, plastic, and tine pitch QFP packages in the type 2 test vehicle.
- A 10 zone convection oven was used for reflowing.
- The first assembled lest Vehicle (TV) using an RMA reflow process was visually inspected and X-rayed to check solder joint quality.
- Ail assemblies were X-rayed
- A reflow profile was also developed for Water Soluble paste based on the manufacturer's recommendation.

Two test vehicles were assembled:

- Type 1, ceramic and plastic BGA packages with nearly 300 1/0s, and,
- Type 2, ceramic and plastic BGA packages with nearly 600 1/0s. Also utilized was a 256 leaded and a 256 plastic BGA package for evaluating and direct comparing manufacturing robustness and reliability.
- Assemblies with water soluble flux were cleaned in an Electrovert H500. Those with RMAs cleaned used Isopropyl Alcohol (IPA) and a 5% saponified.
- All tine pitch QFPs had to be reworked for bridges.

Thermal Cycling

The thermal profile and temperature cycling ranges used at the two facilities were significantly different. 'i'he JPL cycle (cycle A) ranged -30 to 100°C and has increase/decrease heating rate of 2°C and dwell of about 20 minutes at hot temperature to assure near complete creeping. The duration of each cycle is 82 minutes.

Boeing' .cycle (cycle B) ranged -55 to 125°C. It could be also considered a thermal shock since it uses three region chamber, hot, air temp, and cold. Heating and cooling rates are non linear and varies between 10 to 15 °C/min and dwells at extreme temperatures of about 20 minutes. The total cycle lasts approximately 68 minutes. BGA test vehicles were continuously monitored through a LabView system at both facilities.

'i'he criterion for an open solder joint specified in IPC-SM-785, Sect. 6.0, was used as guideline to interpret electrical interruptions. It read: "Solder joint open circuit is defined as the first interruption

of electrical continuity that is confirmed by 9 additional interruptions within an additional 10% of the cyclic life". Generally once the first interruption was observe, there were more than 9 additional interruptions within the 10% of the cycle life. In several instances, one or a few early interruptions were not followed by additional interruptions till significantly later stages of cycling. This was specifically more evidenced for plastic packages.

Damage Monitoring

For conventional SMT solder joint, the pass/fail criterion at JPL relies on visual inspection at 10x to 50x magnifications. For BGA, only edge balls, those not blocked by other components, were visually inspected. A series of single assemblies cut from the test vehicles were used for both visual and SEM inspection to better define visual criterion for ;icccptancc/rejection of solder joints as well as monitoring damage mechanism and progress under different cycling environment.

Figure 1 shows representative SEM and cross-sectional micrographs for CBGA 625 after 300 of cycles A. Package side eutectic solder joint interface, top photos, and board interface, bottom photos, were included. The left photo, is one of the corner pin with the maximum DNP (Distance to Neutral Point).

Figure 2 shows the package interface, top, and board interface after 150 thermal cycle B. The left photos are those for the corner pin and the rights are for its neighbor pin.

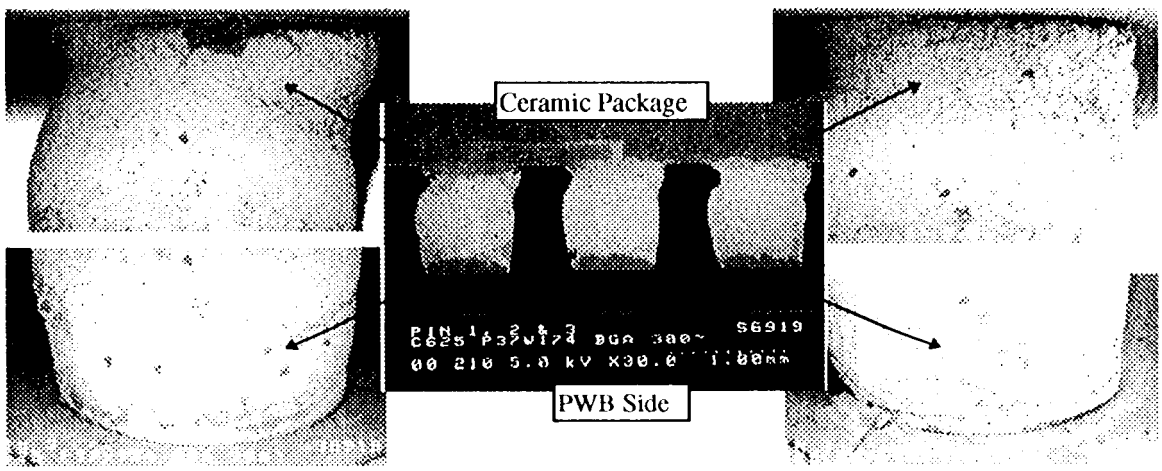

Figure 1 SEM and Cross-section photos for CBGA 625 after 300 cycles, -30°C<->100°C.

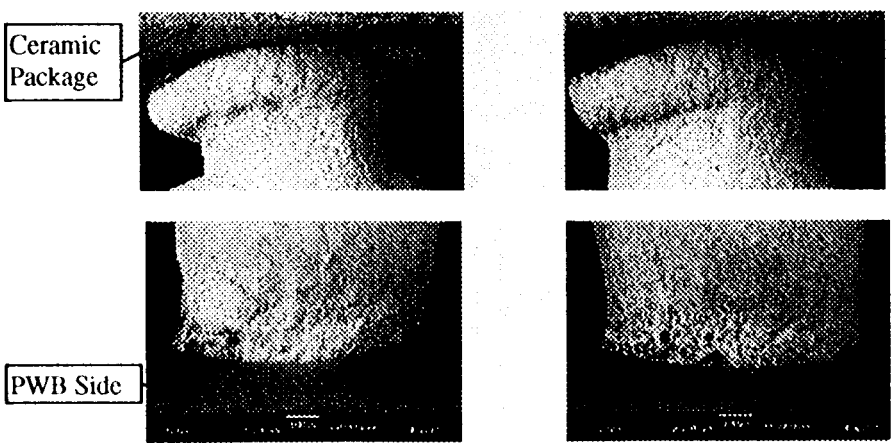

Figure 2 SEM Photos for CBGA625 after 150 Cycles, -55°C<->125°C.

Thermal Cycling Results

CBGA 625/Cycle B

Figure 3 includes cycles to first solder joint failure for CBGA 625 1/0s assemblies on polyimide and FR-4 PWBs with different surface finishes as well as different solder volumes. Results are for those cycled at JPL. The cycles to failure were ranked from low to high and failure distribution percentiles were approximated using median plotting position, $F_i = (i-0.3)/((n+0.4)$.

Often, two-parameter Weibull distributions have been used to characterize failure distribution and provide modeling for prediction in the areas of interest. The cycle to failure data in log-log were fitted in a straight line and the two Weibull parameters were calculated.

For this case, the 2P Weibull scale and shape parameters were 424 and 9.1. Five highest points, four representing those with Ni/Au and one with high solder volume, were excluded in order to get a better fit to data.

CBGA625/Cycle B

Figure 4 shows results of first cycles to failure for CBGA625 assemblies on FR-4 and Polyimide. All assemblies on polyimide showed higher cycles to failure and are shown with different symbols in plots. One assembly on FR-4 showed unexpectedly very high cycles to failure (398). This data point was not included in the plot.

PBGA 313 and SBGA352/Cycle A & B

Figure 5 shows cycles to first failure for PBGA 313 and SBGA352 subjected to Boeing cycle. The most current PBGA313 assemblies failed under cycle B condition are also included in the plots for comparison. Weibull parameters will be generate when all failure data are gathered.

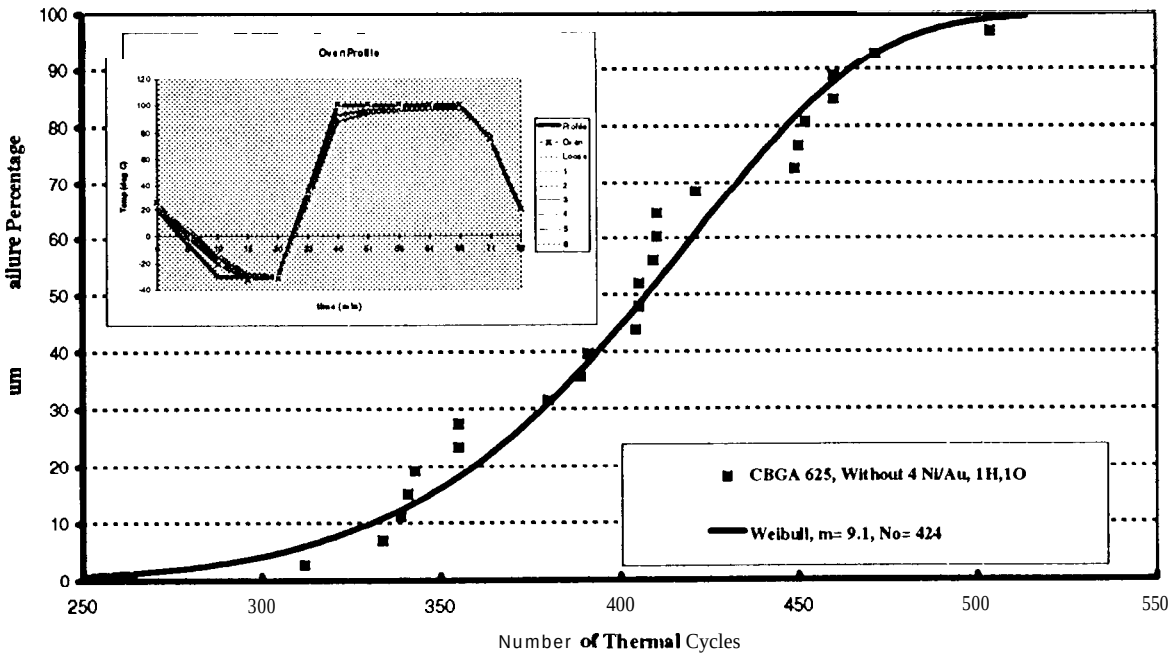

Figure 3 Cumulative Failure Distribution Data and Weibull Plot for CBGA 625 I/O Assemblies Subjected to -30°C<->100°C with 82 minute duration (Cycle A)

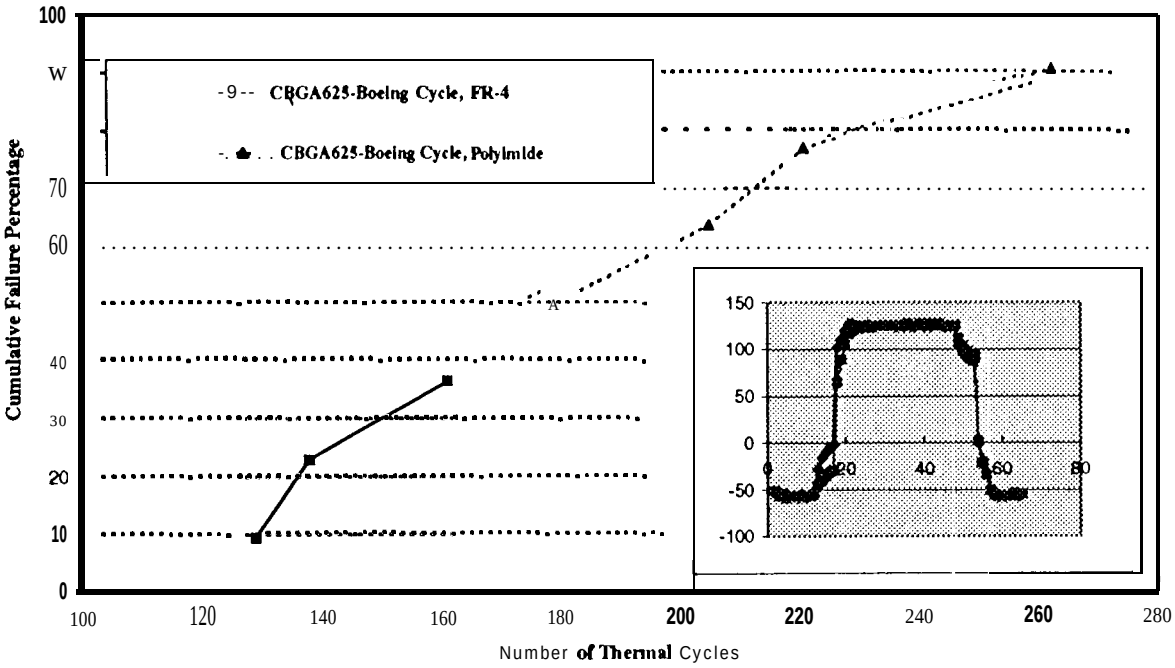

Figure 4 Cumulative Failure Distribution Data Plot for CBGA 625 I/O Assemblies Subjected to -55°C<->125°C (Cycle B) with 68 Minute Duration

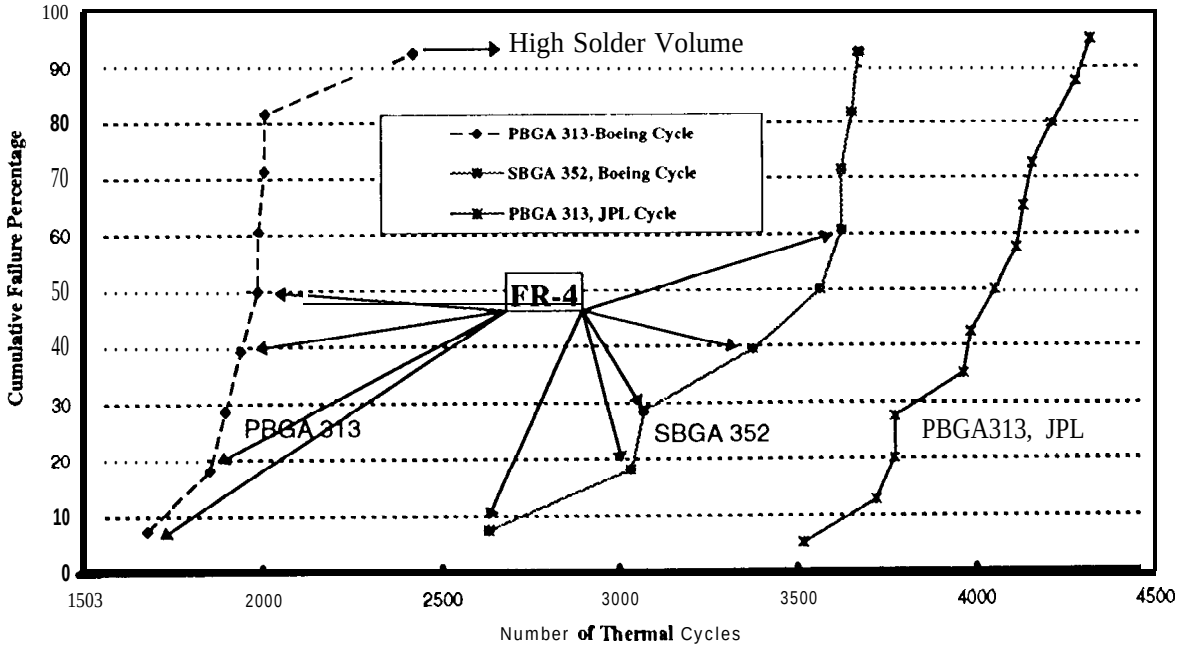

Figure 5 Cumulative Cycling to Failure Data for P 3GA 313 Assemblies (Cycles A&B) and SBGA352 (Cyc e B)

Conclusions

- As expected, ceramic packages failed much earlier than their plastic' counterparts because of their much larger CTE mismatch on FR-4/Polyimide boards. Cycles to electrical failure depend on many parameters including cycle temperature range and package size (1/0).

. Ceramic packages with 625 1/0s were first to show signs of failure among the ceramic (CBGA361) and plastic packages (SBGA560, SBGA352, 0MPAC352, and PBGA256) when cycled to different temperature ranges.

. Joint failure mechanisms for assemblies exposed to two cycling ranges were different. Ceramic assemblies cycled in the range of -30°C to 100"C (A) showed cracking initially at both interconnections with final separation generally from the board side through eutectic solder. The board side joint showed signs of pin hole formation prior to cracking and complete joint failure. 'I'his failure mechanism is similar to those reported in literature for O°C to 100°C thermal cycles.

- For -55°C to 125°C cycle (B), ceramic package failed through interface of package and eutectic solder with signs of significant creeping, "racheting" effect, and solder grain growth. The board side solder creeping and cracking were much milder.

- For cycle B, there were a clear distinction between cycles to failure of ceramic 625 1/0 on FR-4 and Polyimide whereas this was not the case of those of cycle A condition. Cycles to failure differences could be due to closer glass transition temperature (Tg) of FR-4 to cycle B's maximum cycling temperature of 125°C.

. Coffin Manson relationship need to be modified to include the effect of higher temperature exposure and heating/cooling rate to be able to project failure from cycle A to B condition. Differences in physics of failure mechanisms for CBGAs under two conditions may invalidate such projections.

- The PBGA with 313 1/0, full arrays and depopulated, among the PBGAs were first to fail at both cycling ranges. It has been well established that this configuration with balls under the die is not optimum from reliability point of view.

- Solder volume is generally considered to have negligible effects on reliability. One PBGA 313 package that was assembled with high solder paste volume under cycle B exposure showed the highest number of cycles to failure. This will be assessed when data for cycle A become available.

. The 352 SBGA with no solder balls under the die showed much higher cycles to failure than PBGA 313 when subjected to cycle B condition.

. For cycle B conditions, plastic package assemblies, PBGA 313 and SBGA352, on polyimide generally failed at higher cycles than those on FR-4.

REFERENCES

1. R. Ghaffarian, "Area Array Technology Evaluation for Space and Military Applications", The 1996 International Flip Chip, Ball Grid Array, TAB and Advanced Packaging Symposium Proceeding, Feb. 13-16, 1996.

2. R. Ghaffarian, "CBGA/PBGA Package Planarity and Assembly Reliability", The 1997 International Flip Chip, Ball Grid Array, TAB and Advanced Packaging Symposium Proceeding, Feb. 17-19, 1997.

ACKNOWLEDGMENTS

The research described in this publication is being carried out by the Jet Propulsion I aboratory, California Institute of Technology, under a contract with the National Aeronautics and Space Administration.

Special thanks to Sharon Walton at JPL and David Cowen and Kevin Griffith at Boeing for monitoring the environmental testing at JPL. We would like to acknowledge the in-kind contributions and cooperative ef forts of BGA consortium team members including: P. Barela, K. Bonncr, K. Yet, S. Bolin, C. Bodie, *JPL;* M. Andrcws, *ITRI*; S. 1.ockwood, M. Sirncus, P. Drake, *HMSC*; *I.* Sterian, B. Houghton, *Celestica*; M. Ramkumar, *RIT*; *S*. Levine, R. Lecesse, *Altron*; P. Mescher, *AMKOR*; W. Goers and J. Mearig, *EMPF*; *M. Cole,* A. Trivedi, *IBM*; and T. Tarter, *AMD*; F. Schlieper, C. Walquist, *Nicolet*; R. Dudley, R. Balduf *View Engineering.* Our deepest appreciation to others who had been or are being contributors to the progress of both programs.